Optimizing GEO Belt Observation Through Analytical Methods and the Traveling Salesman Problem

Shashanka A G
Digantara Research and Technologies Pvt Ltd
Ananthu Krishna S, Tanveer Ahmed
Digantara Research and Technologies Pvt Ltd

ABSTRACT

Observing and cataloguing satellites in GEO Belt is a crucial endeavour for space satellite tracking, collision avoidance, and space situational awareness applications. However, the efficient and comprehensive observation of satellites within the GEO region presents significant logistical challenges due to the vast number of satellites and the need for precise observational planning. Traditional methods of satellite observation often involve static telescope positioning or sub optimal manual scanning techniques, which can be time-consuming and inefficient. Moreover, given the dynamic nature of satellite orbits and the sheer number of satellites in the GEO belt necessitate innovative approaches to optimize observational strategies. As a response to these challenges, optimising the observation by reducing the number of locations to look in the night sky using analytical methods, offers a systematic approach for cataloguing satellites within the GEO belt. By integrating the principles of the Traveling Salesman Problem (TSP) with analytical methods and telescope technology, we aim to minimize the transition time or slew between observation targets while maximizing data acquisition efficiency along optimised observational path.

Keywords: Traveling Salesman Problem, GEO Belt Observation, Analytical Methods, Object Cataloguing, Satellite Observation, Telescope Efficiency, SSA, Guided Local Search, Sky division.

1. INTRODUCTION

The Geostationary Earth Orbit (GEO) Belt, located approximately 35,786 km above Earth's equator, is a vital region hosting numerous communication, weather, and navigation satellites. Accurate observation and cataloguing of these satellites are essential for satellite tracking, collision avoidance, and space situational awareness. Traditional methods of satellite observation, such as static telescope positioning or manual scanning techniques, are often inefficient due to the vast number of satellites and the dynamic nature of their orbits. Surveying the GEO belt is a critical task for monitoring the population of satellites and space debris, ensuring the safety and sustainability of this valuable orbital region. Traditionally, telescopes have played a central role in this surveillance effort, employing a range of methods to detect, track, and characterize Resident Space Objects (RSOs) in GEO.

Optical telescopes are the most widely used instruments for GEO surveys, leveraging visible light to capture the reflected signatures of RSOs. Through techniques such as wide-field surveys and time-exposure imaging, optical systems can effectively identify and monitor objects as they traverse the GEO belt. The use of long exposure times allows telescopes to capture the light trails of moving objects, providing critical data on their orbital parameters. Radar systems have also been employed, particularly high-power radars capable of detecting objects at GEO altitudes. Although traditionally more effective for lower orbits, these systems can provide complementary data by actively emitting radio waves and analyzing the reflected signals from RSOs. The high power required for GEO radar tracking, however, limits its widespread use. Infrared telescopes offer another method of GEO surveillance, detecting the thermal emissions of objects in space. This approach is particularly useful for identifying faint or dark objects that are difficult to observe in visible light. By capturing thermal signatures, infrared systems can enhance the detection and characterization of RSOs, especially during night-time observations.

Additionally, photometric and astrometric observations are employed to gather detailed information about the physical and orbital characteristics of GEO objects. Photometry measures the brightness variations of RSOs, offering insights into their rotation and surface properties, while astrometry provides precise positional data, essential for accurate orbit determination.

Together, these traditional methods form the foundation of GEO surveillance, enabling continuous monitoring and assessment of the orbital environment. As space traffic in GEO continues to grow, these techniques remain crucial for maintaining the safety and operational efficiency of this congested region. Several ground-based infrastructures and agencies are dedicated to this task, each employing specific strategies to detect, track, and characterize Resident Space Objects (RSOs) and space debris.

The United States Space Surveillance Network (SSN), a key player in GEO monitoring, operates a global network of radar and optical sensors to maintain continuous surveillance. By conducting regular scans and integrating data into a comprehensive catalog, the SSN tracks thousands of RSOs with high precision. Similarly, the European Space Agency (ESA), through its Space Debris Office, utilizes the Space Debris Telescope in Tenerife, Spain, for systematic sky surveys focused on GEO. ESA's strategy emphasizes cataloging and tracking debris alongside operational satellites, contributing to international databases and enhancing global GEO surveillance. The Russian Space Surveillance System combines optical telescopes and radar systems across the Russian Federation to monitor the GEO belt, emphasizing continuous observation and cataloging. China's Space Surveillance and Tracking (SST) System also plays a significant role, utilizing ground-based radar and optical telescopes to provide comprehensive coverage with a focus on refining orbital data. Additionally, international collaborations like the International Scientific Optical Network (ISON) enhance GEO monitoring by coordinating global observatories. ISON employs a distributed survey strategy, with observatories focusing on different GEO segments to optimize data collection. These agencies and infrastructures use a mix of wide-field surveys, targeted observations, and continuous monitoring to maintain accurate catalogs of objects in the GEO belt, thereby mitigating collision risks and ensuring the long-term sustainability of this critical orbital region.

As of epoch June 1 2024, more than 1000 objects are present in the GEO belt region which includes both geo-stationary and geo-synchronous objects. The objects in the day wise TLE catalogue are classified as GEO objects based on the definitions from Spacetrack recent ELSETS page [7] i.e., $0.99 <= \text{Mean Motion} <= 1.01$ and $\text{Eccentricity} < 0.01$.

The current paper presents an innovative approach that integrates analytical methods with the Traveling Salesman Problem (TSP) to optimize the observational strategies for satellites in the GEO belt. By minimizing observation time and maximizing data acquisition efficiency, our approach aims to enhance the overall effectiveness of satellite cataloguing.

2. OBSERVATION RUN SETUP

2.1 Daily Motion of RSOs in GEO region

The geosynchronous satellites occupy a narrow band of inclinations and ascending nodes resulting from exploitation of natural orbit perturbations by geosynchronous satellite station keeping maneuvers as described by [3]. The distinctive patterned behavior of geosynchronous satellites is primarily influenced by the deliberate use of perturbation forces from the Sun, the Moon, and Earth's oblateness. These luni-solar and J2 geopotential perturbations exert a torque on the satellite's orbital plane due to the net out-of-plane force component acting on the object. This torque leads to a correlated periodic variation in the inclination and ascending node of each geosynchronous satellite.

Unlike the sinusoidal motion of objects in declination versus right ascension space, geosynchronous objects exhibit vertical movement in latitude versus longitude. This movement traces out a narrow figure-eight pattern as a result of orbit perturbations.

The space debris in the geosynchronous ring precesses around the Laplace plane. The effects of the second zonal harmonic of the Earth's gravitational potential and the second harmonics of the luni-solar perturbations dominate the precession of the orbital plane of space debris in the geosynchronous ring [1].

Reference [11] made a correlation between the inclination i and RAAN Ω given by Equation 1 closely matching with the statistical distribution of evolution of space debris at different epoch.

$$\cot\Omega = \cot\alpha \ \tan\left(\frac{i}{2}\right) \tag{1}$$

where α is the inclination of the Laplace plane is around 7.4°.
The Theoretical daily motion of the geographic latitude and longitudes of the space objects can be represented as described in [11]:

$$\tan\phi = \tan i \ \sin\left(\lambda + \theta_G - \Omega\right) \tag{2}$$

where ϕ is latitude, i is inclination, λ is longitude, θ_G is Hour angle in radians.
The TLE data of the GEO objects for a particular day is extracted from SpaceTrack [7] and ϕ-λ of these actual objects are plotted along with theoretical ϕ-λ at a particular epoch 1 June 2024 16:00:00 UTC as in Figure 1.

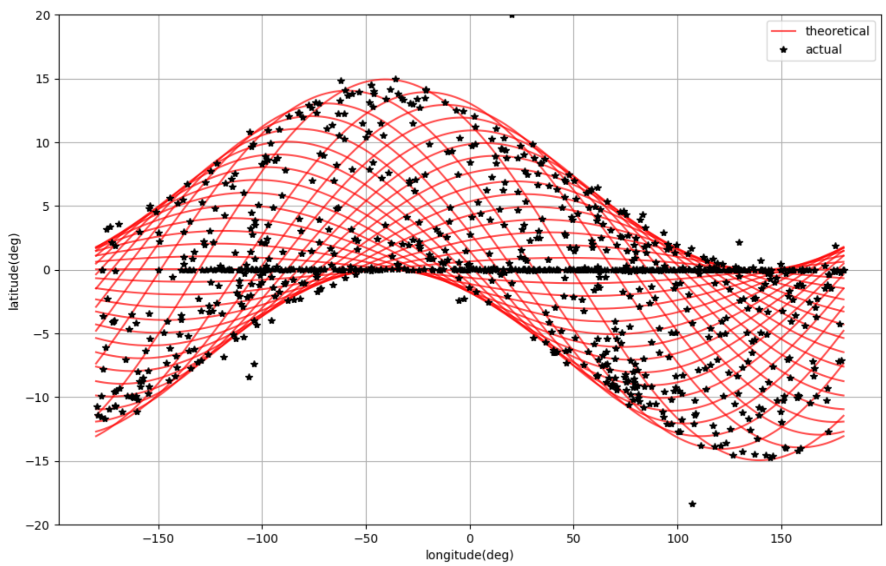

Fig. 1: The theoretical daily motion of geographic latitude and longitude of space objects overlapped with actual objects at same epoch

The theoretical daily motion matches perfectly with actual daily motion of RSOs in the GEO belt region. The theoretical daily motion of ϕ and λ can be used to limit the search areas of RSOs in the geosynchronous ring effectively.

But the GEO belt shape in ECEF frame changes with time with a period of 24 hours. From a location on earth, only a certain part of the GEO belt is visible, and it appears to move between +/- 15° latitude. As the belt is not static in the local sky, there is a need to redefine the grid at regular intervals. Based on Number of grid points a FOV can cover over a orbital inclination range of 15° and the telescope observation time period at each grid, the time of readjustment of grid is decided. These zones of interest are stitched in time throughout the entire operational duration of telescope.

These time adjusted latitude-longitude zones are converted to azimuth-elevation cells based on the location of the observation on the earth.

2.2 Equal Area Sky Subdivision and Filtering GEO region

Several methods can be used to partition the Local sky hemisphere into observation cells. Equal angle division, despite its seeming simplicity, is made up of areas of the sky with larger cell densities. Having a large number of cells at the zenith has drawbacks. For instance, the GEO belt passes through the local sky zenith in the case of an equatorial ground station. Therefore, to swiftly scan the sky without overlaps, equal area sky division is used. We utilise the Equal Area sky subdivision in order to handle the large observational field.

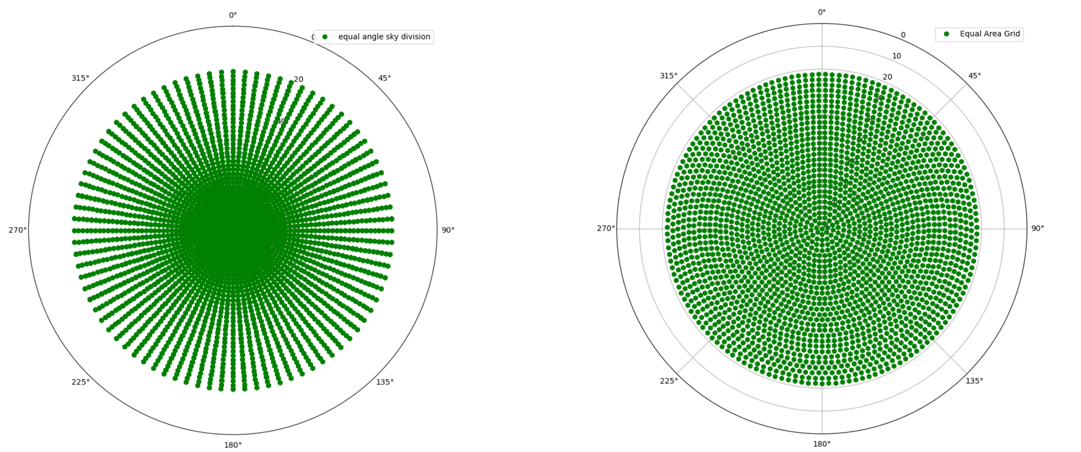

(a) Equal Angle sky division with minimum elevation constraint of 20°

(b) Equal Area sky division with minimum elevation constraint of 20°

Fig. 2: Comparison between Equal angle and Equal area sky divisions

A tessellation is made up of a collection of flat figures that fills the surface entirely, leaving no spaces or overlaps. Reference [2] discussed about the procedures in order to cut a hemisphere into an imposed number of equal-area cells which can be applied to local sky, allowing for a systematic approach to cover the entire GEO belt. The local Sky is represented as Azimuth-Elevation angle domain in a polar coordinate system. As the tessellation of hemisphere is different to that of a disk. The relation between the radius of a disk and elevation angle as given by Eq 3 is used to convert hemispherical cells to cells on disk.

$$r_i = 2\ \sin\left(\frac{v_i}{2}\right) \tag{3}$$

$$\left(\frac{r_i}{r_{i-1}}\right)^2 = \frac{k_i}{k_{i-1}} \tag{4}$$

Where the disk is divided into N circular rings. After the introduction of the ring i with external radius r_i and internal one r_{i1}, the number of cells inside the external circle is equal to k_i. v_i is the corresponding elevation angle of the projected disk radius r_i.

The Local sky with a minimum elevation angle of 20° is filled with Equal area grid as shown in Figure 2. However, not all grid points are relevant to our observation goals. We filter these points to focus only on those corresponding to the GEO belt.

$$v_i = v_{i-1} + 2\ \sin\left(\frac{v_{i-1}}{2}\right)\sqrt{\frac{\pi}{K_{i-1}}} \tag{5}$$

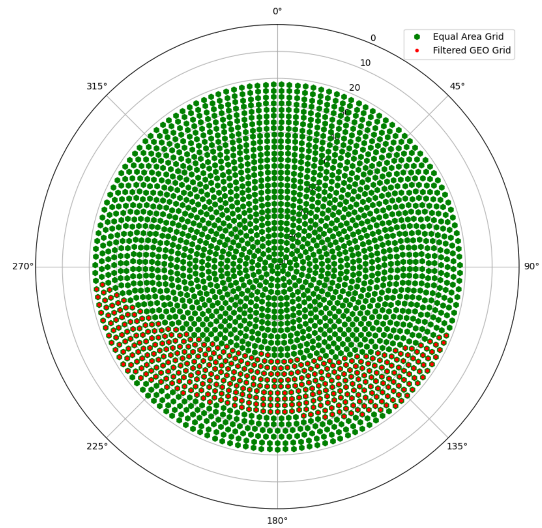

Fig. 3: Filtered GEO belt among the equal area sky grid from a ground observation latitude of 35°.

These sky filled equal area cell centers i.e., grid points are overlapped with time adjusted azimuth-elevation theoretical daily-motion and the equal area cells corresponding to the theoretical daily-motion are filtered based on neighbourhood identification as shown in Figure 3.

2.3 Solving Travelling Salesman Problem for Telescope Observation Scheduling

With a filtered set of Equal area grid points, we face the challenge of efficiently planning the telescope's path. The Travelling Salesman Problem (TSP) is a well-known NP-hard optimization problem that requires finding the shortest possible route that visits a set of cities and returns to the starting point. In the domain of telescope observation scheduling, the TSP framework is particularly valuable for optimizing the sequence of SSA observations, minimizing the transition time or slew between observation targets, while maximizing the scientific value of the observations.

In this context, each observation target is analogous to a city in the TSP, and the goal is to determine the optimal sequence of observations that reduces the total slew time between these targets. Reference [8] discusses about the guided local search (GLS) technique and its application to travelling salesman problem, where the author concludes that GLS performs equally well when compared to other specialised methods while outperforming classic variants of general optimisation techniques. Reference [9] also reports that the GLS algorithm outperforms or compares very favorably with well-known and established optimization techniques such as simulated annealing and tabu search. Hence GLS technique is chosen to the optimize the travelling salesman problem in the following sub sections.

2.3.1 Data Preparation

The method begins by converting the azimuth and elevation inputs of the targets into a list of locations, each represented as a tuple of azimuth and elevation coordinates.

2.3.2 Distance Calculation

The distance between each pair of locations is calculated, which corresponds to the angular distance the telescope must move. This is crucial for minimizing the total slew time. Haversine formula is used to calculate the great circle distance between two lookout angle pairs.

Let θ be the angle between the two points $[(Az_i, El_i), (Az_j, El_j)]$ on local sky hemisphere as shown in Fig 4. The

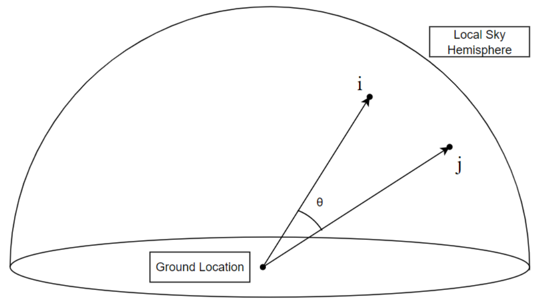

Fig. 4: Local sky hemisphere

haversine of this angle is given by,

$$hav(\theta) = hav(\Delta El) + \cos(Az_i)\ \cos(Az_j)\ hav(\Delta Az) \tag{6}$$

where haversine function is given by,

$$hav(\theta) = \left(\frac{1-\cos\theta}{2}\right) \tag{7}$$

Using Equations 6 and 7, the angle between the lookout angles pairs(θ) is given by,

$$\theta = \arccos\left(\cos\Delta El - \cos Az_i\ \cos Az_j\ (1-\cos\Delta Az)\right) \tag{8}$$

2.3.3 Data Management

The problem is defined by specifying the telescope's starting zone, analogous to a depot in vehicle routing, with a single telescope taking the role of a vehicle. A Routing manager handles the allocation of telescope pointing across different zones in the sky, ensuring that the telescope starts and ends its observation at a specific starting zone. Unlike the conventional Traveling Salesman Problem, where the path returns to the same starting point, this approach is tailored for scanning the sky based on the daily motion of the GEO belt, optimizing the telescope's path through various observation zones without the need to return to the initial zone.

2.3.4 End to End TSP

In order to solve this problem, the TSP must be tweaked in order to start and end at defined points. This can be achieved by adding a hypothetical location whose distance between the start and end points is zero. This additional point acts as a barrier connecting start and end points, so that the algorithm provides solution path that starts with defined end point and ends at the depot.

2.3.5 Path Optimization with Guided Local Search

The method uses search algorithms such as Path cheapest arc to find an initial solution. The Path cheapest arc strategy is a greedy heuristic that builds an initial solution by repeatedly adding the cheapest arc to the current route. It starts with an arbitrary node and iteratively adds the closest (in terms of angular distance) unvisited node until all nodes are included in the route.

To find a better solution, a more advanced search strategy, called guided local search (GLS) is applied using the following procedure:

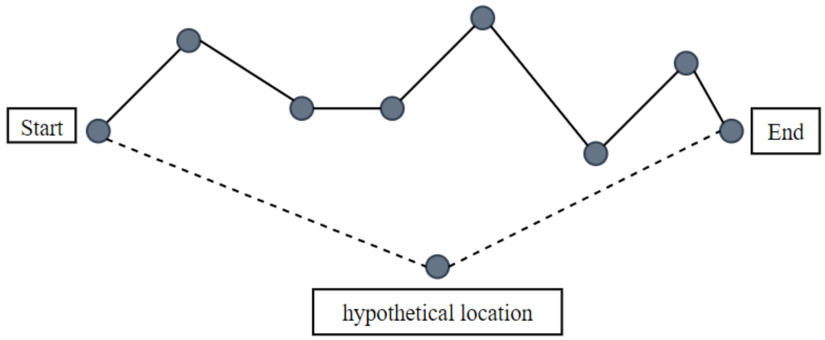

Fig. 5: End to End Travelling Salesman Problem

1. **Initialization**:
   - **Start**: Begin with an initial feasible solution for the TSP, typically generated by a heuristic like Nearest Neighbor or Greedy.
   - **Set Initial Penalties**: Initialize the penalty values for each edge in the solution to zero.
   - **Calculate Initial Cost**: Compute the total cost of the initial solution (sum of distances).
2. **Local Search Phase**:
   - **Apply Local Search**: Perform a local search method such as 2-opt to attempt to improve the current solution by exploring neighboring solutions.
   - **Check for Improvement**: If the improved solution is found, update the current solution and continue the local search or else proceed to the GLS penalty update.
3. **Guided Local Search (GLS) Phase**:
   - **Calculate Augmented Cost**: For each edge in the TSP tour, calculate the augmented cost by adding the original cost and a penalty.
   - **Identify Features to Penalize**: Identify the most "unfavorable" edges (those contributing most to the augmented cost).
   - **Update Penalties**: Increase the penalties for the identified edges.
   - **Modify Solution**: Use the updated penalties to guide the local search in a new direction, encouraging the search to avoid previously overused edges.
4. **Termination**: Based on maximum iterations limit, stop the algorithm and return the best solution found or return to the Local Search Phase with the modified solution.

2.3.6 Final path

The algorithm returns the final TSP tour, which is the best solution found after applying GLS and local search. The final optimal path always ends with the defined end point because of the End to End TSP constraint. This ensures that the telescope's schedule is both efficient and effective.

2.3.7 Advantages of TSP in Telescope Scheduling

- **Optimality**: The TSP ensures that the telescope follows the most efficient path, minimizing the time spent moving between targets. This is critical in time-sensitive SSA observations.
- **Scalability**: The method can handle a large number of targets, making it suitable for complex observation schedules.

2.4 Implementation and Data Acquisition

The optimized observational path derived from the TSP solution is then implemented using telescope technology. As the telescope follows this path, it systematically observes and records GEO objects, maximizing data acquisition efficiency.

3. GEO BELT SURVEY

In general, object tracking mode has the limitation of potentially missing numerous objects as they move across the field of view, which lowers the efficiency of observation for routine operations. In a GEO region survey, not only are perfectly geostationary objects visible, but also quasi-geostationary objects, zero-inclination semi-geostationary satellites like GPS, and various objects moving along the equator.

Sidereal tracking is a better approach for ensuring that all stars remain fixed in the image. Building on our previous strategy, we can employ sidereal tracking during a sequence of exposures. In Chen Zhang et.al., [10], the author divided the GEO region into 72 - 6° x 6° fields other than 7° x 7° fields, considering the vignetting of the optics. On each field several 4 sec exposures are taken which lasts 3 minutes, and it costs 18 min for the whole region survey using 12 telescopes. A single telescope would have costed around 216 min to complete the whole region survey. The telescope used is a custom APO refractor with 280mm effective aperture and 300mm focal length, and sensor has 3056 x 3056 12-micron pixels, makes it 51.9 mm in diagonal.

The number of grid points needed to cover the GEO belt reduces from 72 block grid [10] to 57 block time adjusted filtered Tregenza grid indicating a 20.833% reduction in region to be covered for a FOV of 36 sq deg as shown in Figure 6. Out of all the GEO objects observable in the night sky, 79.56% coverage is achieved with a coverage rate of 0.88% per minute.

In order to check the effect of the telescope field of view on number of equal area grid points to be surveyed in the local sky, several simulations are run and tabulated as shown in Table 1. It can be seen how having low F-number, large field of view systems can be a huge advantage for GEO belt survey applications, significantly reducing the time required for survey.

FOV (deg)	Number of Equal Area Grid points
2	392
3	181
4	116
5	79
6	57
7	49
8	38
9	27

Table 1: Number of Equal Area Grid points required to cover the GEO belt visible from a location based on FOV.

The CONUS GEO belt region [4] subtends 120 degrees E-W and 30 degrees N-S, or 3,600 square degrees centered N-S on the projected declination of the GEO orbits. The telescope used for observation is a Celestron C-14 – a 14-inch (355 mm) diameter catadioptric telescope operated with a Starizona HyperStar prime focus corrector to provide an effective focal length of 684 mm. The 2048 detector pixels subtend a field of view of 1.8 x 1.8 degrees, or 3.53 square degrees on the sky per exposure.

The CONUS GEO belt mosaic requires 1020 images, and 163 minutes to complete with one sensor with a dwell time of 9.6s. These observation runs are carried out from New Mexico (35 Latitude). Considering the same latitude as reference and similar specifications of telescope, the current TSP based method needs 447 grid points (for 1.8 x 1.8

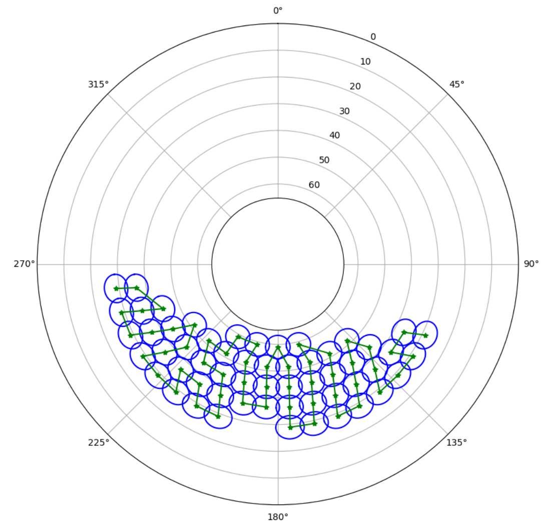

Fig. 6: Pointing path of GEO grid with 6°x6° FOV

degrees FOV) i.e., a total duration of 72 minutes (9.6s dwell time) to complete the GEO belt survey in CONUS GEO region showing a reduction in duration by nearly half. The final path with FOV grid is shown in Figure 7.

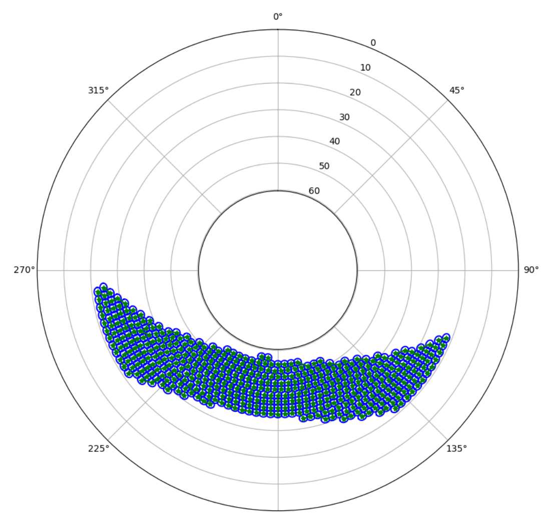

Fig. 7: Pointing path of GEO grid with 1.8°x1.8° FOV

4. CONCLUSION AND FUTURE WORK

The integration of analytical methods with TSP for optimizing GEO belt observation presents a novel and effective solution to the logistical challenges faced in this field. By systematically reducing the observation region and optimizing the telescope's path, we can achieve higher coverage rates and minimize observation time.

The proposed methodology not only improves the efficiency of current observational techniques but also provides a scalable solution that can be adapted to different observational needs and technological advancements. The promising results of our preliminary implementation highlight the potential for broader application and further refinement. This methodology significantly reduces the observational region and optimizes the telescope's path minimizing transition times, resulting in enhanced efficiency and coverage rates.

The preliminary results demonstrate the effectiveness of our approach, achieving a 20.833% reduction in the observation region. This method contributes to the improvement of space situational awareness and satellite management capabilities, ensuring the continued safety and functionality of satellites in Earth's orbit. However, the integration of observational constraints and the need for real-time updates present significant challenges. Addressing these challenges requires advanced optimization techniques capable of handling the complexity and dynamic nature of modern SSA observation schedules.

In practical applications, telescope observation scheduling is often subject to constraints such as time windows when targets are visible, weather constraints, priority zones and accounting for noise sources such as moon, milkyway etc. The current method can be extended to address these issues as a part of future work.

5. REFERENCES

[1] RR Allan and GE Cook. The long-period motion of the plane of a distant circular orbit. *Proceedings of the Royal Society of London. Series A. Mathematical and Physical Sciences*, 280(1380):97–109, 1964.

[2] Benoit Beckers and Pierre Beckers. A general rule for disk and hemisphere partition into equal-area cells. *Computational Geometry*, 45(7):275–283, 2012.

[3] KS Capelle and J Sharma. Geosynchronous satellite orbit pattern: improvements to sbv geosynchronous search. In *Proceedings of the 2000 Space Control Conference. Citeseer*, pages 29–42. Citeseer, 2000.

[4] John T McGraw, Peter C Zimmer, and Mark R Ackermann. Multiple observing modes for wide-field optical surveillance of geo space. In *Advanced Maui Optical and Space Surveillance Technologies Conference*, page 24, 2016.

[5] Akhter Mahmud Nafi and David Geller. Practical survey strategies for geo from a single ground based observatory. In *AAS/AIAA Astrodynamics Specialist Conference*, 2018.

[6] Peter Roy Tregenza. Subdivision of the sky hemisphere for luminance measurements. *Lighting Research & Technology*, 19(1):13–14, 1987.

[7] U.S. Space Command. Space-track. `https://www.space-track.org/`, 2024.

[8] Christos Voudouris and Edward Tsang. Guided local search and its application to the traveling salesman problem. *European journal of operational research*, 113(2):469–499, 1999.

[9] Christos Voudouris, Edward PK Tsang, and Abdullah Alsheddy. Guided local search. In *Handbook of metaheuristics*, pages 321–361. Springer, 2010.

[10] Chen Zhang, Y Ping, and C Zhao. Ches: A rapid all-sky survey system for ssa. In *Proceedings of the The Advanced Maui Optical and Space Surveillance Technologies Conference, Wailea, Maui, HI, USA*, pages 11–14, 2018.

[11] Chang-Yin Zhao, Ming-Jiang Zhang, Sheng-Xian Yu, Jian-Ning Xiong, Wei Zhang, and Ting-Lei Zhu. Variation ranges of motion parameters for space debris in the geosynchronous ring. *Astrophysics and Space Science*, 361:1–16, 2016.